Spacecraft Contamination under Simulated Orbital Environment

R.W. Phillips,* L.U. Tolentino,† and S. Feuerstein‡
The Aerospace Corporation, El Segundo, Calif.

Volatile condensable material (VCM) measurements on a number of spacecraft materials have indicated that contamination rates onto surfaces at subambient temperatures cannot be predicted from standard outgassing tests, particularly where long-term exposures are involved. Contamination rates may depend markedly on temperature differentials between source and collector, the collection temperature, the source geometry, and the exposure time. Contamination rates also may be influenced by solar irradiation. The results of this study were obtained on a new VCM facility that overcomes many deficiencies experienced in earlier designs and permits accurate simulation of space environmental conditions. Advantages of the present system include an oil-free high-vacuum chamber (10^{-8}—10^{-9} Torr), source temperatures from ambient to 125°C, collection temperatures from −140° to +125°C, total mass-loss measurements, in situ VCM mass measurements with use of an internal-temperature-compensated quartz-crystal microbalance, in situ vacuum ultraviolet irradiation of either the specimen or of the collected VCM, and infrared identification of the VCM by multiple internal reflection spectroscopy. The system also features automated data acquisition and data processing.

I. Introduction

In order to carry out their assigned missions, satellites not only must function with very high reliability, but they must continue to do so for long periods of time. As time passes, the prevention of contamination on critical thermal control and optical surfaces becomes more difficult. In some applications, a small change in the solar absorptance, α_s due to contaminant effects can hamper seriously the performance of a mission. It is essential, therefore, that the importance of various sources of contamination be ascertained in order that corrective action can be initiated. Recent flight data indicate that the contamination problem is still significant.[1]

A number of spacecraft programs have thermal control surfaces that must operate at cryogenic temperatures and may be in direct line of sight with contaimination sources. Even surfaces out of direct line of sight of out-gassing material may receive condensate.[2] Extrapolation of room-temperature collection data to cryogenic conditions is difficult, particularly if long-term exposure effects are sought. Accurate measurements of contamination under conditions that simulate long-term orbital environments are needed particularly to estimate operational lifetimes for satellites with critical surfaces operating at cryogenic temperatures.

Since problems caused by contaminant films on critical surfaces first were discovered, numerous studies have been carried out to determine the outgassing properties of spacecraft materials.[3-7] The standard method of determining the acceptability of a candidate spacecraft material is to heat the sample in vacuum at 125°C for 24 hr.[3-5] It has been proposed that the total mass loss and the material depositing on a 25°C surface from this heated source be less than 1% and 0.1%, respectively, of the original sample mass. This method is excellent for the rapid screening of materials proposed for spacecraft use, but rates of outgassing and condensation cannot be determined. A calibrated microbalance system has been developed which allows the measurement of outgassing rate either isothermally or with a monotonic increase in temperature.[6] However, the rate of condensation or possible re-evaporation of the condensate cannot be measured. Another system provides more information by continuously monitoring the mass loss of the material as well as the mass gain of the condensate.[7] In addition, reflectance and scattering measurements of the contaminated surfaces are obtained. Unfortunately, no provision is available for identifying the contamination, and the system suffers from a non-line-of-sight configuration between source and collector. The preceding systems also have one or more of the following additional disadvantages: they are not oil free, outgassing occurs during evacuation, cryogenic collection of VCM is not possible, and they do not provide for in situ simulated solar irradiation of either the source or the collector.

In this paper, a new automated space simulation facility that overcomes most of the cited dificiencies of earlier designs is described. Measurements are discussed, and the results of a number of outgassing experiments carried out on this facility are analyzed.

II. Instrumentation

A. Chamber

The VCM apparatus (Fig. 1) is an oil-free stainless-steel vacuum chamber that is pumped by a liquid-nitrogen-cooled molecular sieve sorption pump and a Perkin-Elmer/Ultek 100-liter/sec ion pump. There are no polymeric sealants or insulation within the chamber. Seals are made with copper gaskets and glass-to-metal seals; electrical insulation is achieved by encircling bare copper wire with ceramic beads. In contrast to previous systems, a tubular cryoshield at −196°C extends around the outgassing source (the specimen) and up to just in front of the collectors. This arrangement restricted the experiments to measuring only line-of-sight contamination.[2] Demand of liquid nitrogen through the cryoshield was controlled by a novel two-tank sequencer.[8]

B. Collection Apparatus

1. Double Quartz Crystal Microbalance (DQCM)

The mass sensing element is a 1.5- × 0.75-in. single-crystal wafer of quartz, resonating at 5 MHz, of the type developed by Termeulen et al.[9] Approximately 50 Å of chromium,

Received Oct. 21, 1976; revision received Feb. 22, 1977.
Index categories: Research Facilities and Instrumentation; Materials, Properties of; Spacecraft Testing, Flight and Ground.

*Member of the Technical Staff, Chemistry and Physics Laboratory, The Ivan A. Getting Laboratories.
†Associate Technical Staff, Chemistry and Physics Laboratory, The Ivan A Getting Laboratories.
‡Head, Interfacial Sciences Department, Chemistry and Physics Laboratory, The Ivan A. Getting Laboratories.

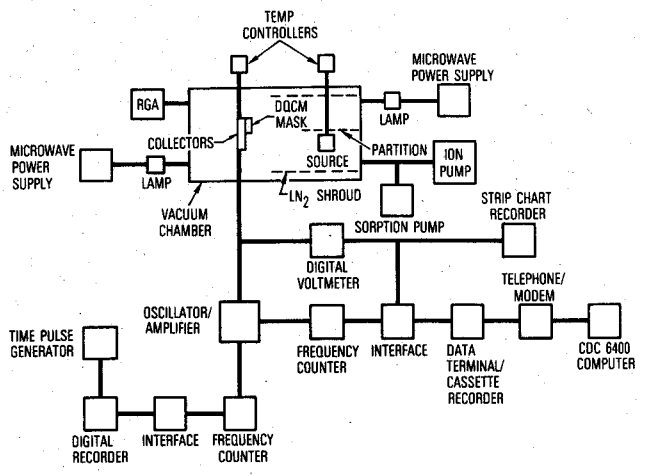

Fig. 1 Block diagram of VCM facility.

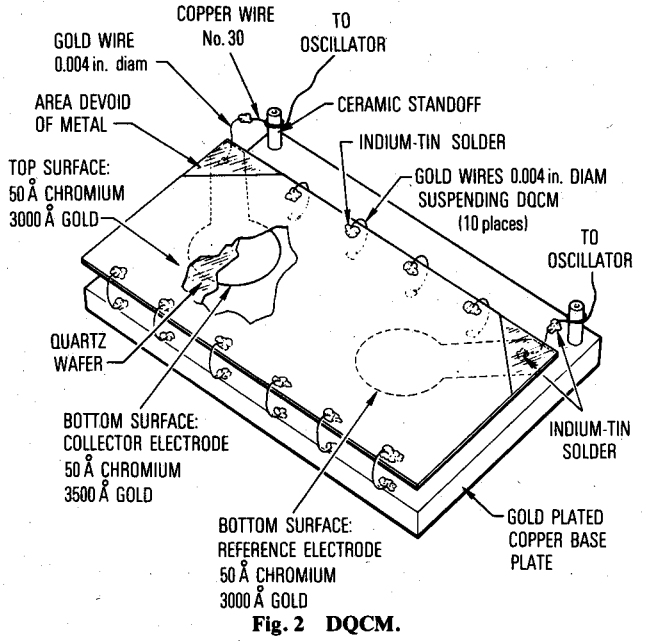

Fig. 2 DQCM.

followed by 3000 Å of gold, is vacuum-deposited onto the quartz to form the collecting and reference electrodes, as shown in Fig. 2. Resonance across both reference and collector sides of the quartz crystal is induced by a Miller oscillator in conjunction with a mixer-amplifier output circuit. In operation, the collector side of the crystal is exposed to mass deposition, whereas the reference side is protected from mass deposition by a mask. It is important to make the collecting electrode more massive than the reference electrode in order to avoid crystal frequency instabilities. Apparently, the active portions of the two crystals have a strong tendency to couple mechanically in the regime of near mass equivalence. An additional 500 Å of gold deposited on the collector side of the crystal generally is sufficient to overcome this problem.

The quartz is suspended from an oxygen-free high-conductivity (OFHC) copper baseplate by using 0.004-in.-diam gold wire, soldered to the front face with indium. Such a mounting minimizes mechanical damping and crystal stress caused by differential thermal contractions.

Two types of AT-cut crystals were used in the present study, one cut at 35° 10′ and the other at 39° 49′. Beat frequency profiles over temperatures of −140° to 25°C showed small shifts that amounted to 30 and 200 Hz, respectively. Absolute shifts were on the order of 13 kHz. These low beat frequency shifts indicate, in effect, that this type of crystal monitor has good inherent temperature compensation. Normally, two crystals must be mounted independently in the same vicinity in order to achieve similar temperature compensation.

Vacuum-evaporated aluminum films of various thicknesses on the monitoring side of the crystal yielded an average mass sensitivity of 58.6 Hz-μg^{-1} $-cm^2$, which is in reasonable agreement with the theoretical value of 57.5 Hz-μg^{-1} $-cm^2$ for an AT-cut 5-MHz quartz crystal.[10]

2. *Internal Reflectance Element (IRE)*

A trapezoidal 45° cut KRS-5 internal reflectance element serves as a collecting substrate for infrared (ir) identification of the condensate. It is located immediately below the quartz crystal microbalance. Infrared spectra were taken after each test, at ambient conditions, on a Perkin Elmer ir spectrometer (model 467) equipped with an IRE holder accessory.

3. *Residual Gas Analyzer (RGA)*

A quadrupole residual gas analyzer (Electronic Associates model Quad 200) also is used for mass identification of the outgassing material (Fig. 1).

C. Temperature Controls

The outgassing source (specimen) holder and the base to which the collectors are attached are made of copper for rapid and uniform temperature accommodation. Source temperatures can be set at −196°C or adjusted between 25° and 125° with a cartridge heater in conjunction with an API (model 503K) temperature controller (API Company) and an iron constantan thermocouple. Temperature control of the collectors can be maintained between −140° and +125°C by controlled heating of the cooled copper base. Heat conduction prevents lower temperatures at the collectors. The collectors and cryoshield temperatures are monitored by copper-constantan thermocouples referenced to a junction at 77K.

D. Vacuum Ultraviolet Sources

Mercury vacuum ultraviolet lamps with Suprasil windows are attached to the test chamber such that either the condensate or the specimen can be irradiated in situ. Power to the lamps is supplied by a Raytheon PGM 10X1 microwave power (2.45 GHz) supply with a "C"-type antenna. The partition prevents direct ultraviolet irradiation of the outgassing source during condensation irradiation. Similarly, the collector base prevents irradiation of the condensate during specimen irradiation. It is necessary to shield the rf antenna properly in order to prevent oscillator instabilities.

The photon flux at a distance of 27.9 cm from the source was measured at $\lambda = 184.9$ and 253.7 nm by using the nitrous oxide actinometer[11,12] and the potassium ferrioxylate chemical actinometer,[13] respectively. Flux densities were calculated to be $\approx 10^{14}$ photons/cm^2 at both primary wavelengths. At these wavelengths, the level of irradiation was calculated to be about 3.1 times the power of the sun.[14]

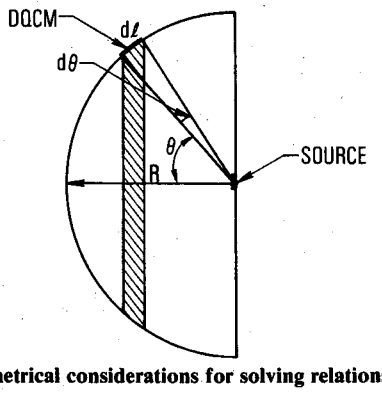

Fig. 3 Geometrical considerations for solving relationship of M_T to M_p.

E. Microprocessor Data-Acquisition System

Changes in the DQCM beat frequencies as material is deposited or re-evaporated from the unmasked side of the crystal are displayed on a Heath digital frequency counter (model SM-104A). The frequency data are recorded directly by a digital printer or indirectly onto a cassette tape for permanent storage. Direct recording is done with a Texas Instruments Silent 700 ASR terminal linked to a CDC 6400 computer system. In this case, the sampling rate is controlled by an Varitel DAC-80 controller coupled to an NLS multichannel scanner. Alternatively, a Hewlett Packard (model 562A) printer can be used to obtain an immediate hard copy of the frequency data. Here, the data subsequently are key-punched and batched through a CDC 7600 computer. Disk files within the CDC 7600 system also are created to permit manipulation of the data into final form and to permit plotting by a multipen Cal-Comp plotter. For the latter acquisition system, a specially built pulse unit controls the data-sampling interval from 1 sec to 1 hr. A 10-min time interval proved to be most convenient. The time pulse generator was protected from transient line signals by using an isolation transformer.

F. Transfer Vessel

A large metal bellows located on the top side of the vacuum chamber is designed for ex situ ultraviolet and visible spectral measurements of the condensate under actual collecting conditions, i.e., low temperature and vacuum. By the compression of the bellows, the collector assembly passes into a latching cover in the base of the chamber. An indium gasket serves as a seal. When the latches are in place, the entire assembly, including the cover (with appropriate optical windows), can be removed from the system after the rest of the chamber has been back-filled with dry nitrogen. This particular feature was not used in this investigation.

III. Experimental

A. Materials and Sample Preparation

The RTV-615 samples, polydimethylsiloxane from General Electric, were prepared in disk form according to aerospace industry standards by mixing 90.9 wt% RTV-615 A polymer and 9.09 wt % RTV-615B curing agent. The RTV-566 sample, polymethylphenylsiloxane from General Electric, was prepared according to aerospace standards by mixing 99.8 wt % RTV-566A polymer and 0.2 wt % RTV-556B curing agent. The Kapton sample, a 3-mil polyimide film, was used as received from the manufacture, DuPont Corporation.

Samples were cured in a desiccator at room temperature for seven days. No effort was made to precondition the samples for humidity and temperature prior to use. The RTV samples were cast directly into a copper mold of disk design and attached directly to the copper specimen holder. The Kapton film was cut to disk size and kept in place by a fastened wire screen.

B. Procedure

Prior to each experiment, the system was baked at 125°C for 48 hr. A vacuum of 10^{-8} to 10^{-9} Torr ultimately was achieved. With the cryogenic shroud at −196°C, background contamination rates were reduced to negligible amounts, ≤ 0.25 pg-cm^{-2} −min^{-1}, as measured by the frequency of the DQCM at −140°C.

Specimens were attached to the sample holder and fixed into place after first closing off the pumping system and backfilling the chamber with dry nitrogen. Sorption pumping for approximately 10 min reduced the chamber pressure to $\approx 10^{-4}$ Torr, after which the sample was frozen to −196°C. This freezing procedure was necessary in order to prevent premature outgassing. At this point, the chamber was switched from sorption pumping to ion pumping. The cryogenic shroud, the DQCM, and the IRE then were cooled to their respective temperatures.

Once the vacuum had been attained and the system temperature equilibrated, the source was heated to the desired temperature as rapidly as possible. Equilibrium source temperature was achieved in a matter of minutes. The total mass of material collecting on the DQCM was measured every 10 min by automatically recording the DQCM beat frequency. Total collecting time varied from 1 to 5 days. Irradiations were started as indicated in Table 1.

Each experiment was terminated by allowing the DQCM and IRE to warm slowly to 25°C. Subsequently, the LN_2 shroud was also allowed to warm to room temperature. Then, the system once again was backfilled with dry nitrogen, the IRE was removed, and an ir spectrum was taken. It was

Table 1 VCM facility outgassing conditions

Experiment	Material	Specimen			Outgassing Time, hr	Target UV Irradiated
		Mass, g	Thickness, 10^{-1} cm	Temp, °C		
1	RTV-615	0.5702	1.10	23	60.0	
				100	120.8	
2	RTV-615	0.5342	1.03	23	96.7	
3	RTV-615	0.5369	1.04	100	24.3	
4	RTV-615	0.5030	0.973	100	111.8	Collectors[a]
5	RTV-615	0.4657	0.900	100	64.3	
6	RTV-615	3.1279	6.05	100	37.7	Collectors[b]
7	RTV-615	0.5306	1.03	100	65.2	Collectors[b]
8	RTV-615	0.5577	1.08	100	114.7	Source[b]
9	RTV-566	1.3018	1.70	100	95.3	Collectors[b]
10	Kapton	0.0563	0.076	23	24.0	

[a] Irradiation started during VCM collection. [b] Irradiation started at $t = 0$.

assumed that the contaminant film on the IRE was representative of the film formed at low temperature. This assumption may be justified somewhat by noting that 1) the more volatile material is deposited first, 2) the first several layers of an adsorbed film are difficult to remove even by thermal treatment, and 3) the irradiated condensate, which undergoes less re-evaporation when warmed, has a similar ir spectrum to that of the unirradiated condensate. Total mass loss of the specimen was determined simply by weighing the sample on an analytical balance (±0.5 mg) before and after the experiment.

IV. Theoretical Considerations

It is necessary to delineate the relationship between the mass of material as collected on the DQCM and the total VCM emitted by the source. For this purpose, equations were derived by analogy to the field of illuminating engineering.[15] Derivations of the equations are given in some detail because previous derivations of similar relationships were either superficial or did not apply to the present geometry.[16]

The quantity of material emitted at an angle θ, M_θ, is related to that emitted perpendicular to a planar outgassing source, M_P by Knudsen's cosine law:

$$M_\theta = M_p \cos\theta \tag{1}$$

However, to relate the mass per unit area on the DQCM [$(m/A)_{\mathrm{DQCM}}$] to the total VCM, M_T, a relationship between M_T and M_p must be established. Consider first the situation where the DQCM is affixed to the inside surface of a hemispherical cup that encloses the outgassing source at its center (Fig. 3). If the source-to-collector distance R is assumed to be sufficiently large, then to a first approximation one may write, from the inverse square law

$$\left(\frac{m}{A}\right)_{\mathrm{DQCM}} = \frac{M_p \cos\theta}{R^2} = \left(\frac{\mathrm{d}m}{\mathrm{d}A}\right)_{\mathrm{DQCM}} \tag{2}$$

Now by integrating the total mass deposited over the available hemispherical surface, one can relate M_T to M_p, i.e.,

$$M_T = \int_0^m \mathrm{d}m = \int_0^A \frac{M_p \cos\theta \, \mathrm{d}A}{R^2} \tag{3}$$

The standard method of evaluating this integral is to consider $\mathrm{d}A$ as the area confined to a ring of width $\mathrm{d}l$ and of radius $R\sin\theta$ (Fig. 3). Since $\mathrm{d}l = R\mathrm{d}\theta$ and the circumference of the ring is $2\pi R\sin\theta$,

$$M_T = 2\pi \int_0^{\pi/2} M_p \sin\theta \cos\theta \, \mathrm{d}\theta = \pi M_p \tag{4}$$

In order to calculate $(m/A)_{\mathrm{DQCM}}$ for the case where the source and the DQCM are nonparallel (Fig. 4), an angle correction ψ (the angle between the normal to the DQCM surface and the radius R) must be used. Again, R is large relative to the dimensions of the source. In this case, substitution of M_T/π for M_p in Eq. (2) and multiplication by $\cos\psi$, to take into account the collector angle dependency, yield

$$\left(\frac{\mathrm{d}m}{\mathrm{d}A}\right)_{\mathrm{DQCM}} = \frac{M_T \cos\theta \cos\psi}{\pi R^2} \tag{5}$$

For a source size that may be comparable to R, the relationships between $(\mathrm{d}m/\mathrm{d}A)_{\mathrm{DQCM}}$ and M_T is found as follows. In the case of a large disk source, the disk is divided up into a series of concentric rings such that each ring has an area of $\mathrm{d}\sigma = 2\pi x \mathrm{d}x$ (Fig. 5). For each disk, R once again is large relative to the dimensions of the source; therefore Eq. (5) applies. Now, $M_T = M\sigma$, where M is the mass emitted from the source per unit area, and σ is the total surface area of the source.

For the case where both source and collector surfaces are parallel and coaxial, the substitution of

$$\sigma = \int_0^\sigma \mathrm{d}\sigma \quad x = L\tan\theta \quad \mathrm{d}x = L\sec^2\theta \, \mathrm{d}\theta \quad \psi = \theta$$

into Eq. (5) yields

$$\left(\frac{\mathrm{d}m}{\mathrm{d}A}\right)_{\mathrm{DQCM}} = 2M\int_0^\theta \cos\theta\sin\theta \mathrm{d}\theta = M\sin^2\theta \tag{6}$$

or

$$\left(\frac{\mathrm{d}m}{\mathrm{d}A}\right)_{\mathrm{DQCM}} = \frac{Mr^2}{r^2 + L^2} \tag{7}$$

From the relationship $M = M_T/\sigma$ and the fact that σ is the area of the source, i.e., πr^2, $M = M_T/\pi r^2$ can be substituted into Eq. (7). Since $L^2 >> r^2$ for this facility ($L = 17.4$ cm, $r = 1.27$ cm), then

$$\left(\frac{\mathrm{d}m}{\mathrm{d}A}\right)_{\mathrm{DQCM}} = \frac{M_T}{\pi L^2} \tag{8}$$

It can be shown, by consideration of Knudsen's law, that the distribution of condensate on the DQCM was uniform to within 0.04% (active electrode area ~1 cm). Thus, $(\mathrm{d}m/\mathrm{d}A)_{\mathrm{DQCM}}$ may be replaced by $(m/A)_{\mathrm{DQCM}}$; hence,

$$(m/A)_{\mathrm{DQCM}} = M_T/\pi L^2 \tag{9}$$

for the VCM facility described herein.

V. Results and Discussion

A. Volatile Condensable Material (VCM) and Total Mass Loss (TML)

The experimental conditions and results for the three samples tested (RTV-615, RTV-566, and Kapton) are given in Tables 1 and 2. The VCM given in units of milligrams per steradian, was calculated by multiplying the observed mass per unit area on the DQCM by the square of the source-to-

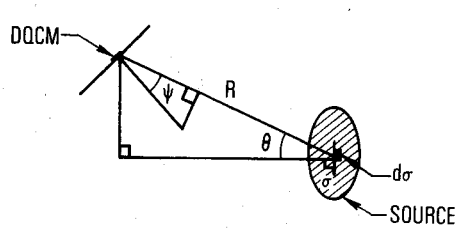

Fig. 4 Geometrical considerations for solving relationship of mass on DQCM to M_T when source and collectors are nonparallel.

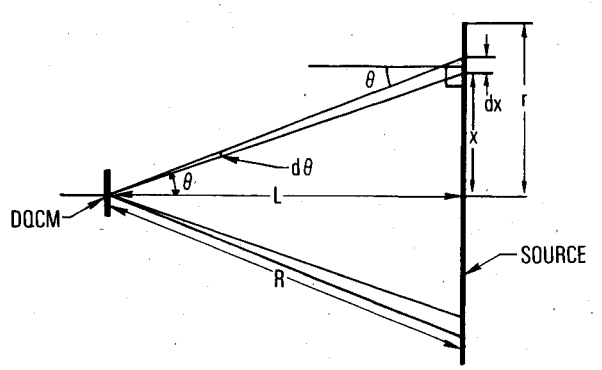

Fig. 5 Geometrical considerations for solving relationship of mass on DQCM when source is large relative to collector-source distance.

Table 2 Outgassing results

Experiment	Total Mass Loss		Collected Volatile Condensable Material, mg/sr		Total Volatile Condensable Material,[a] mg		Collection Efficiency,	Contaminant Remaining After Warming,
	mg	%	24 hr	Total hr	24 hr	Total hr	%	%[b]
1	9.0 ± 0.5	1.7	0.581[c]	0.843	1.83	2.65	27	7
			1.86[d]	2.60	5.86	8.17	82	
2	8.3	1.6	0.337	0.657	1.06	2.06	25	2
3	7.7	1.4	1.22	1.41	3.84	4.43	58	4
4	9.1	1.8	2.20	2.52	6.93	7.91	87	65
				2.82[e]		8.86	97	
5	8.1	1.7	2.28	2.63	7.15	8.27	102	
6	15.5	0.50	4.19	4.67	13.2	14.7	95	
7	9.6	1.8	2.59	2.90	8.14	9.15	95	92
8	7.6	1.4	2.02	2.26	6.36	7.11	94	34
9	2.8	0.22	0.226	0.308	0.711	0.968	34	<1
10	0.2	0.36	0.157	0.247[f]	0.492	0.777	388	<1

[a] Calculated (see text). [b] Volatile condensable material remaining on the DQCM after warming to 23°C. [c] Source at 23°C. [d] Source at 100°C. [e] Extrapolated value, assuming no irradiation. [f] Source at 23°C for 5.33×10^3 min, then 100°C for 3.02×10^3 min.

collector distance, i.e., $(m/A)L^2$. Equation (9), derived in the preceding section, was used to calculate the total volatile condensable material (TVCM) emitted from the source. The percent volatile condensable material remaining on the DQCM after the collectors were warmed from −140° to 23°C is given in the last column of Table 2.

For the RTV-615 samples, a near mass balance existed between the total emitted VCM as calculated by Eq. (9) and the total mass loss (TML) of the sample. This indicates that little, if any, noncondensable material was emitted by these samples. It also implies that the theoretical derivation is fundamentally correct. Low collection efficiencies (i.e., low TVCM/TML ratios) observed in experiments 2 and 3 resulted from the source being exposed to extended vacuum or heat following the DQCM measurements or both. In particular, experiment 2 was similar to experiment 1 in that the source was heated serially at 23° and then at 100°C. Loss of coolant in the cryoshield during the second portion of experiment 2 precluded VCM measurements when the source was heated. Therefore, only the 23°C VCM results are presented. However, the sample continued to lose mass during the 100°C heating period, and this resulted in the low collection efficiency. The collection efficiency given for experiment 2 nevertheless is correct for the portion measured because almost the same ratio was obtained for the first part of experiment 1.

The high collection efficiency observed for Kapton (experiment 10) can be explained readily by the inherently large error in TML. A collection efficiency greater than 100% indicates that more mass was emitted and collected as VCM than was found by weighing the specimen before and after the outgassing experiment. Apparently, absorbed atmospheric gases lost as VCM from the specimen are regained rapidly on subsequent exposure to the atmosphere.[17] Thus, the measured TML value is too low, and consequently the collection efficiency becomes higher than physically possible.

The low collection efficiency observed for RTV-566 appears to be a result of a relatively high level of noncondensables. A 0.22% TML value for the RTV-566 compares favorably with values of 0.23% and 0.27% reported by others for a similar RTV-566.[18] However, this agreement may be more fortuitous than real (see discussion below).

TVCM percentage values calculated for the three samples tested fell within the expected range of values reported by others, i.e., 1.54% (experiment 5), 0.055% (experiment 9), and 0.88% (experiment 10) vs 0.83%, 0.0 to 0.03%, and 0.03%, respectively.[18] (Percent TVCM was calculated by dividing column 6 of Table 2 by column 3 of Table 1 and

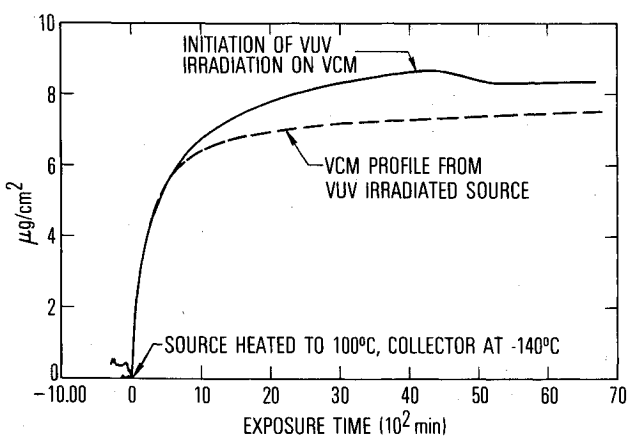

Fig. 6 VCM deposition profiles of RTV-615 (—experiment 4; --- experiment 8).

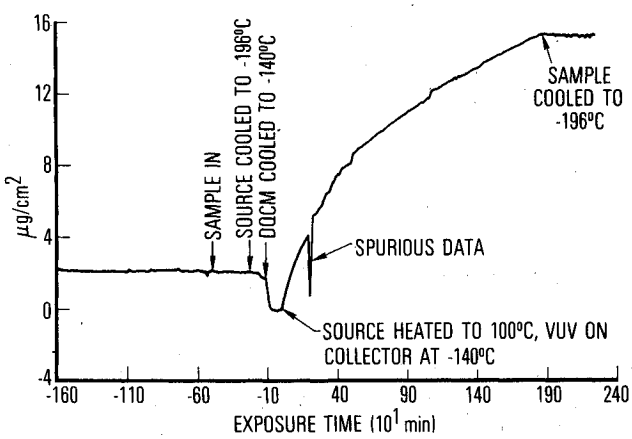

Fig. 7 VCM deposition profile of RTV-615 when collectors were irradiated by Vuv (experiment 6).

multiplying by 100.) The higher levels of TVCM in the present experiments not only may be a consequence of the lower collection temperature (−140° vs 25°C), but they also may be due to differences in sample geometry, as discussed later.

Studies were conducted primarily with RTV-615 because it was readily obtainable and had a sufficiently large outgassing rate that changes due to differing conditions could be observed. Unless stated otherwise, the discussion here concerns the RTV-615 samples. A typical outgassing curve for this material is shown in Fig. 6. It must be pointed out that substantial amounts of material still were outgassing and depositing as VCM for times greater than 24 hr (14.4×10^2 min) at both −140° and 23°C collection temperatures. These results tend to contradict the conclusions made by Muraca and Whittick that nearly all of the VCM is collected in 24 hr from 100- to 200-mg samples.[3] Their conclusions were made on the basis of large-scale outgassing tests called macro-VCM tests, as opposed to the former micro-VCM tests, with 4- to 10-g samples. Their macro-TML values not only are greater than the micro-TML values, in one case by almost 1000%, but the large samples continued to significantly outgas beyond the 24-hr period (Table 3).

The only agreement between the two tests appears in the TVCM values at or near the detection limit of 0.01%, where roundoff errors tend to mask differences. One would have expected the macro-TVCM to increase as the macro-TML increased because, with time, the outgassing material becomes progressively less volatile and thus tends to be collected more efficiently.

Meaningful TML values can be given only if the source geometry also is specified. In Tables 1 and 2, it is evident that, in the case of RTV-615, an increase in the thickness of the outgassing source from 0.103 to 0.605 cm (experiments 6 and 7) decreased the 24-hr TML from 1.61 to 0.44%. A priori, one might have expected the same TML value regardless of sample thickness. The 24-hr TML percentage values were calculated from the ratio of the collection efficiency (column 8, Table 2), the absolute value of the TVCM at 24-hr (column 6, Table 2), and the source mass. Although similar results, i.e., 1.8 vs 0.5%, could have been found in column 3, different outgassing times for the two samples perhaps would have biased the foregoing conclusion. It must be emphasized that most of our samples were equal to or thinner than 0.3 cm, which was the upper limit thickness for the microtests of Muraca.

On the basis of our experiments and our reinterpretation of the data of Muraca and Whittick,[3] we believe that VCM can outgas significantly beyond the 24-hr period, and that the rate of outgassing is diffusion-controlled even for microsamples. It is evident that a sample with a high surface-to-volume ratio will outgas far more rapidly than a sample of similar composition with a low surface-to-volume ratio, because, in the latter case, the outgassing molecules have further to diffuse than in the former. Thus, sample mass should be normalized to a given surface-to-volume ratio in calculating TML and TVCM percentages. This outgassing process will be treated in greater detail in a subsequent paper.

B. Radiation Effects

When vacuum ultraviolet (Vuv) irradiation ($\lambda = 184.9$ nm) of the condensate was initiated after collection already had begun, the mass first decreased and then leveled off (Fig. 6). The decrease in mass was attributable to loss in volatile components caused by photodissociation of the condensate. No significant effects on the VCM deposition profile were observed, however, when the irradiation was started at the same time as the collection (Fig. 7). In this case, the rate of deposition swamped out any small photodissociation effect. It should be noted that, when the source was cooled rapidly to −196°C, the VCM curve immediately flattened out, which indicates that outgassing had ceased. The latter observation verifies that background VCM levels were negligible.

In contrast to the case where the condensate had not been irradiated, the DQCM did not return to near its base frequency upon warming to room temperature (Table 2). Apparently, the condensate was fixed to the surface at the low temperature by the Vuv radiation through polymerization and cross-linking. Visually, the irradiated VCM appeared as a dark square. (Unirradiated VCM was transparent.) Cross-linking reactions were inferred from the broad ir bands and the relative insolubility of the condensate. Darkening and fixing of condensate by solar irradiation also were noted on recent Skylab flights.[19]

The foregoing observations have important implications for the common practice of heating low-temperature critical surfaces to drive off spacecraft contamination. Polymers useful for spacecraft where surfaces are maintained at 25°C or above may be unsatisfactory for those systems that use low temperatures, particularly in cases where such surfaces may be exposed to solar irradiation.

Vuv irradiation of the specimen resulted in the reduction of long-term VCM (Fig. 6). Apparently, the radiation further cross-linked the cured RTV-615. This had the combined effect of reducing the diffusion rate of the VCM from the host material and reducing the vapor pressure of the polymer. The Vuv irradiation of the source also partially fixed the condensate. Most likely, reactive radicals formed in the gas phase reacted when they were deposited onto the collectors. Reflective Vuv irradiation of the condensate, although possible, did not appear likely, because more than one reflection would have been required. An increase in the molecular weight of the outgassing material also appears improbable because the initial outgassing rate was similar to the unirradiated case (Fig. 6), even though the Vuv irradiation had been turned on prior to the time of source heating.

C. VCM Identification

The ir spectra of the collected VCM (RTV-615) had bands at 7.93 μm ($Si-CH_3$), 9-10 μm (Si-O-Si), 11.75 μm ($Si-CH_3$), and 12.5 μm ($Si-CH_3$), indicating a methyl silicone contaminant (Fig. 8).[20] There was no evidence of Si-H (4.4 to 4.8 μm), $SiCH_2Si$ (7.3 μm), or $Si-CH_2-CH_3$ (13.5 to 13.6 μm) linkages.[21]

Cross-linking of the VCM by Vuv irradiation may have occurred by way of scission of the C-H bond on the methyl group, with subsequent formation of $Si-CH_2-CH_2-Si$ structures. This structure has ir absorption bands at 8.85 and 9.5 μm, which would tend to broaden the Si-O-Si ir absorption peaks in the 9- to 10-μm region.[22] Such broadening was, in fact, observed.

The intensities of the ir absorption peaks were related to the amount of volatile condensable material remaining on the collectors after warming to 23°C. Experiments 3, 4, 7, and 8 had 1.2, 24, 8.9, and 2.5 μm-cm^{-2}, respectively, remaining on the DQCM after warmup. The seemingly large amount of remaining condensate for experiment 4 was caused by a temporary failure of the cryoshield during the latter part ($t > 70 \times 10^2$ min, Fig. 6) of the experiment while the collectors were still cold and while the Vuv was still on. In spite of the temporary warming of the cryoshield, the conclusions reached earlier regarding the nature of the effect of Vuv irradiations remain valid. Loss of the cryoshield also was experienced late in experiment 3, a case where the condensate never was irradiated by Vuv. In the latter experiment, however, only a small amount of condensate remained behind after warming. The absolute amount of volatile condensable material remaining on the collectors of experiment 4 provides a good demonstration of the need for cryoshield protection during low-temperature VCM collection. A higher-than-expected level of condensate is just what one would anticipate for a system that uses secondary surfaces warmer than the collectors in a non-line-of-sight configuration.[2]

The ir spectrum and, hence, the composition of condensate may be quite different from that of the parent material from

Table 3 Selected data from Ref. 3

Sample	Macro Tests				Micro Tests	
	Total Mass Loss, %		Total Volatile Condensable Material, %		Total Mass Loss, %	Total Volatile Condensable Material, %
	24 hr	96 hr	24 hr	96 hr	24 hr	24 hr
Epoxi Patch A/B	0.70	1.16	0.01	0.01	1.18	0.01
Micarta 65M25	0.36	0.44	0.01	0.01	0.43	0.00
Teflon FEP 500 A	0.01	0.01	0.01	0.01	0.05	0.05
Eccofoam S	0.21	0.48	0.01	0.01	2.01	0.07
Delrin 150NC10	0.20	0.37	0.01	0.02	0.56	0.06
Hycar 520-67-108-1	1.19	1.24	0.10	0.12	1.90	0.17
Mystik 7452	0.15	0.18	0.06	0.05	0.37	0.04

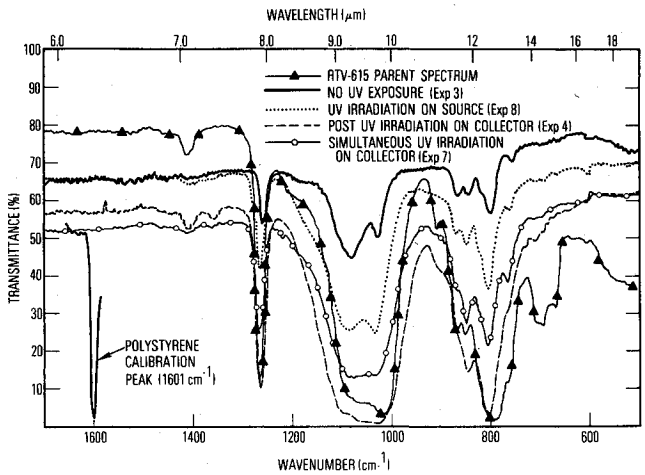

Fig. 8 Infrared spectra (25°C) of RTV-615 VCM and RTV-615 parent material.

which the condensate originated. It should be noted that the ir spectra of the condensate, particularly the spectrum of condensate from experiment 3 in the 9- to 10-μm region, is quite different from that of the parent material in the relative band intensities. Thus, irradiation of deposited VCM, compared with that of thin films prepared from parent material (pseudo-VCM), may yield quite different results and conclusions.[23]

Mass spectral analysis of the chamber gases taken with the RGA revealed no significant peaks over and above background levels. The lack of mass spectral peaks may have been a consequence of the non-line-of-sight placement of the RGA relative to the outgassing source. In addition to this possible deficiency, the outgassing levels may have been below the RGA detection limit. Our findings are in agreement with the observations of Goldsmith and Nelson, who also found that cold collectors, because of their time-integrating effect, can detect compounds missed by an RGA.[24]

VI. Conclusions

An improved instrument for accurately measuring the rate of contamination from materials under a variety of space environments has been developed. The apparatus is particularly unique because either the outgassing specimen or the condensate may be irradiated in situ while the collectors are maintained at cryogenic temperatures.

Vacuum ultraviolet irradiation of the cryodeposit from outgassed RTV-615 produces a highly cross-linked condensate that is nonvolatile at room temperature. In the absense of irradiation, however, most of the cryodeposit is sufficiently volatile at room temperature to evaporate. Irradiation of the RTV-615 specimen not only reduces the rate of long-term outgassing but also decreases the condensate volatility.

Specimen geometry rather than mass appears to control the rate at which a sample tends to outgas. Thus, outgassing two specimens of the same composition and of the same weight for a given period of time may lead to widely differing total mass loss and volatile condensable material percentages. This difference results because diffusing molecules will take longer to reach the surface for an outgassing specimen with a small surface-to-volume ratio than for one that has a large surface-to-volume ratio.

Acknowledgment

This work was supported by the U.S. Air Force under Contract No. F04701-76-C-0077. The authors wish to thank P.D. Fleischauer and D.F. Hall for their critical reviews, which aided in clarification of the text. They also wish to thank R.D. Brink for significant contributions to the early design of the VCM facility and W.J. Kalinowski for invaluable assistance in interfacing the data-acquisition system to the VCM facility.

References

[1] Rantanen, R.O., Bareiss, L.E., and Ress, E.B., "Determination of Space Vehicle Contamination," *Proceedings of Evaluation of Space Environment on Materials,* Toulouse, France, June 1974, p. 211.

[2] Kan, H.K.A., "Desorptive Transfer: A Mechanism of Contaminant Transfer in Spacecraft," *Journal of Spacecraft and Rockets,* Vol. 12, Jan. 1975, p. 62.

[3] Muraca, R.F. and Whittick, J.S., *Polymers for Spacecraft Application Final Report,"* Stanford Research Inst. Project ASD-5046, Jet Propulsion Lab. Contract 950754, Menlo Park, Calif., Sept. 15, 1967.

[4] "Method of Test for Total Mass Loss and Collected Volatile Condensable Materials from Outgassing in a Vacuum Environment," Standard E595-77, American Society for Testing and Materials, Philadelphia, Pa.

[5] Fisher, A. and Mermelstein, B., "GSFC Micro-Volatile Condensable Materials System for Polymer Outgassing Studies," NASA-

TMX-65399, Goddard Space Flight Center, Greenbelt, Md., Oct. 1969.

[6] Jensen, L.B., McCauley, G.B., and Honma, M., "Vacuum Thermogravimetric Analysis System for Determination of Continuous Weight Change and Total Condensable Materials," *Non-Metallic Materials, Selection, Processing and Environmental Behavior,* Vol. 4, National SAMPE Technical Conference Series, Palo Alto, Calif., Oct. 1972, p. 179.

[7] Poehlman, H.C., "Outgassing and Contamination Properties of Prospective Apollo Telescope Mount Materials," *Non-Metallic Materials Selection, Processing and Environmental Behavior,* Vol. 4, National SAMPE Technical Conference Series, Palo Alto, Calif., Oct. 1972, p. 197.

[8] Shepherd, J.R. and Corbin, R.L., "Two-tank Sequencer for Control of Liquid Nitrogen Withdrawal," *Review of Scientific Instruments,* Vol. 46, Dec. 1975, p. 1702.

[9] Termeulen, J.Ph., Van Empel, F.J., Hardon, J.J., Massen, C.H., and Poulis, J.A., "The Use of Double Oscillating Quartz Crystals in Mass Determination," *Progress in Vacuum Microbalance Techniques,* Vol. I, edited by T. Gast and E. Robens, Heyden and Son, Ltd., New York, 1972, p. 41.

[10] Neidermayer, R., Gladkick, N., and Hillecke, D., "Thin-Film Thickness Measurements with a Quartz Oscillator," *Vacuum Microbalance Techniques,* Vol. 5, edited by K.H. Behrndt, Plenum Press, New York, 1966, p. 217.

[11] Zelikoff, M. and Aschenbrand, L.M., "Vacuum Ultraviolet Photochemistry, Part I. Nitrous Oxide at 1470A," *Journal of Chemical Physics,* Vol. 22, Oct. 1954, p. 1680.

[12] Greiner, N.R., "Photochemistry of N_2O Essential to a Simplified Vacuum-Ultraviolet Actinometer," *Journal of Chemical Physics,* Vol. 47, Dec. 1967, p. 4373.

[13] Calvert, J.G. and Pitts, J.N., *Photochemistry,* Wiley, New York, 1966, p. 783.

[14] Thekaekara, M.P., "The Solar Constant and the Solar Spectrum Measured from a Research Aircraft," NASA TR R-351, Goddard Space Flight Center, Greenbelt, Md., Oct. 1970, p. 75.

[15] Moon, P., *The Scientific Basis of Illuminating Engineering,* Dover, New York, 1961, Chap. IX.

[16] Holland, L. and Steckelmacher, W., "The Distribution of Thin Films Condensed on Surfaces," *Vacuum,* Vol. 2, Oct. 1952, p. 346.

[17] Hait, P.W., "The Application of Polyimide to Ultra-High Vacuum Seals," *13th National Vacuum Symposium of the American Vacuum Society,* San Francisco, Calif., Oct. 26-28, 1966.

[18] "Compilation of VCM Data of Non-Metallic Materials," NASA Lyndon B. Johnson Space Center, Houston, Texas, April 1976, rev. H.

[19] Lehn, W.L. and Hurley, C.J., "Results of the Polymeric Films Skylab DO24 Experiment," Air Force Materials Lab., Wright-Patterson Air Force Base, TR 75-165, Ohio, 1975.

[20] Haslam, J., Willis, H.A., and Squirrel, D.C.M., *Identification and Analysis of Plastics,* Butterworth, London, 1972, 2nd ed.

[21] Delman, A.D., Landy, M., and Simms, B.B., "Photodecomposition of Polymethylsiloxame," *Journal of Polymer Science,* Vol. 7, Pt. A1, Dec. 1969, p. 3375.

[22] Curry, J.W., "The Synthesis and Polymerization of Organosilances Containing Vinyl and Hydrogen Joined to the Same Silicon Atom," *Journal of the American Chemical Society,* Vol. 78, April 1956, p. 1686.

[23] Fleischauer, P.D. and Tolentino, L.U., "The Far Ultraviolet Photolysis of Polymethyphenlysiloxane Films on Quartz Substrates," *Proceedings of the Seventh Conference on Space Simulation,* Los Angeles, Calif., Nov. 12-14, 1973, NASA-SP-336, 1973, p. 645.

[24] Goldsmith, J.C. and Nelson, E.R., ASTM/IES/AIAA Space Simulation Conference, Gaithersburg, Md., Sept. 14-16, 1970, National Bureau of Standards, NBS 336, Washington, D.C., Oct. 1970.